Supporting information

Nanosized Cu-MOF induced by graphene oxide and enhanced gas storage capacity

Shuang Liu [a,c], Lixian Sun [a, b*], Fen Xu[b,d*], Jian Zhang [a], Chengli Jiao [a], Fen Li [a], Zhibao Li [a,c], Shuang Wang [a,c], Ziqiang Wang [a,c], Xia Jiang [a,c], Huaiying Zhou [b], Lini Yang[e] and Christoph Schick[f]

[a] *Materials and Thermochemistry Laboratory, Dalian Institute of Chemical Physics, Chinese Academy of Sciences, Dalian 116023, China.*
[b] *Graduate School of Chinese Academy of Sciences, Beijing 100049, China.*
[c] *Faculty of Chemistry and Chemical Engineering, Liaoning Normal University, Dalian 116029, China.*
[d] *Department of Material Science & Engineering, Guilin University of Electrical Technology, Guilin, 541004, China.*
[e] *Department of Chemistry, Liaoning University, Shenyang, 110036, China*
[f] *Institute of Physics, Universität Rostock, Rostock D-18059, Germany*

** Corresponding author. Tel./Fax: +86-411-84379213.*
E-mail address: lxsun@dicp.ac.cn (Lixian Sun); xufen@lnnu.edu.cn (Fen Xu)

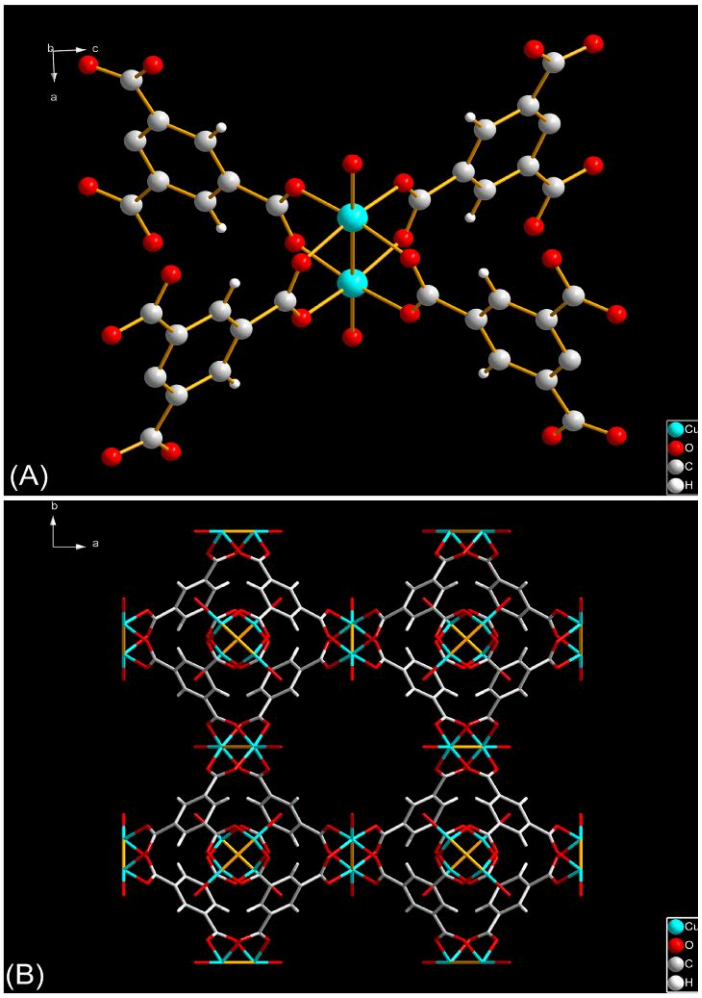

Fig. S1 (A) Dicopper (II) tetracarboxylate building block for Cu-BTC;
(B) $[Cu_3(BTC)_2(H_2O)_3]n$ polymer framework viewed down the [100] direction, showing nanochannels with fourfold symmetry.

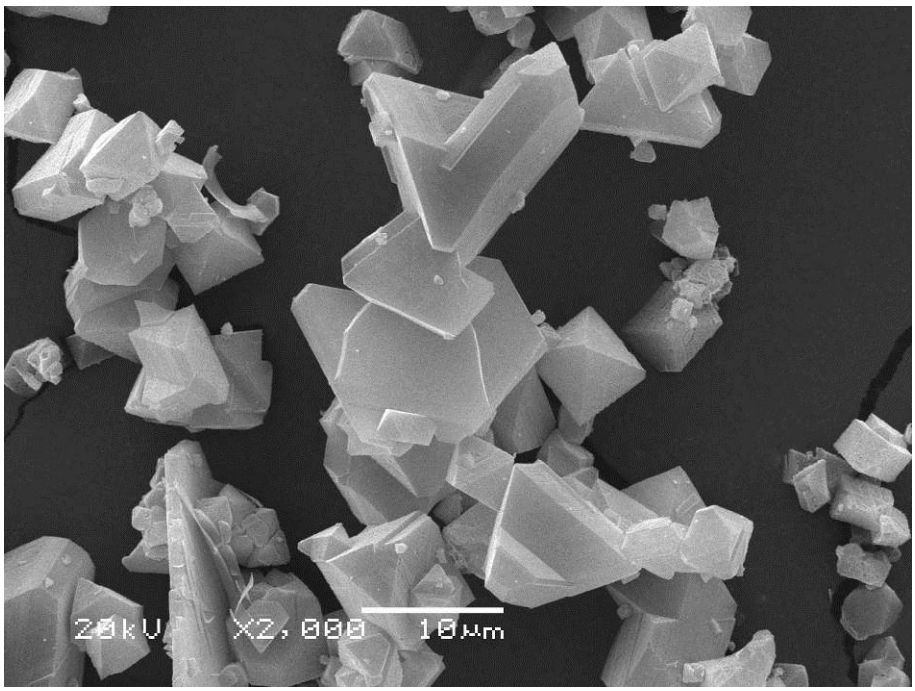

Fig. S2 SEM micrograph of Cu-BTC crystals.

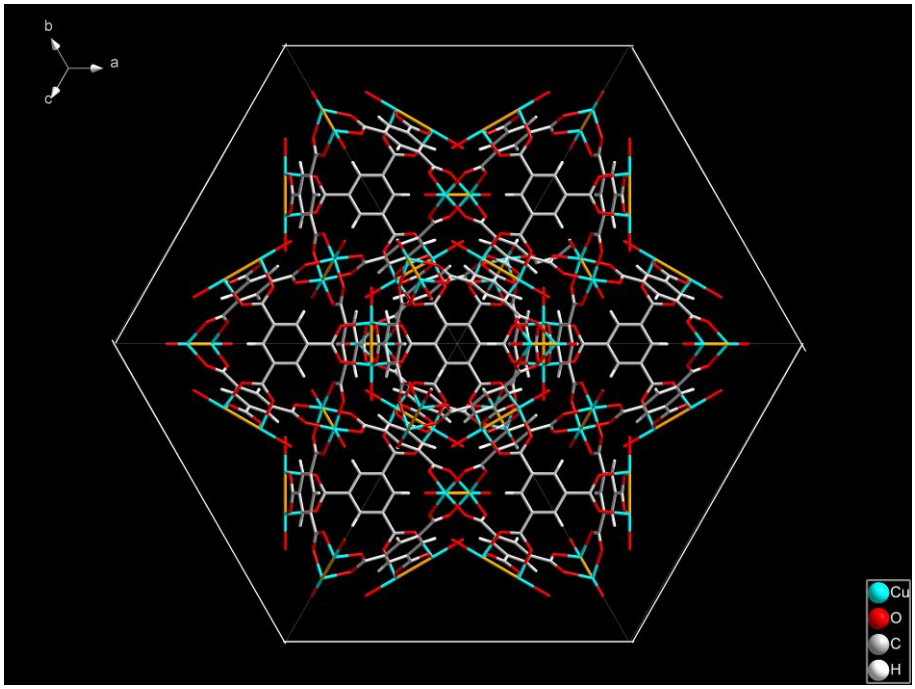

Fig. S3 $[Cu_3(BTC)_2(H_2O)_3]_n$ polymer framework viewed down the [100] direction, showing a hexagon.

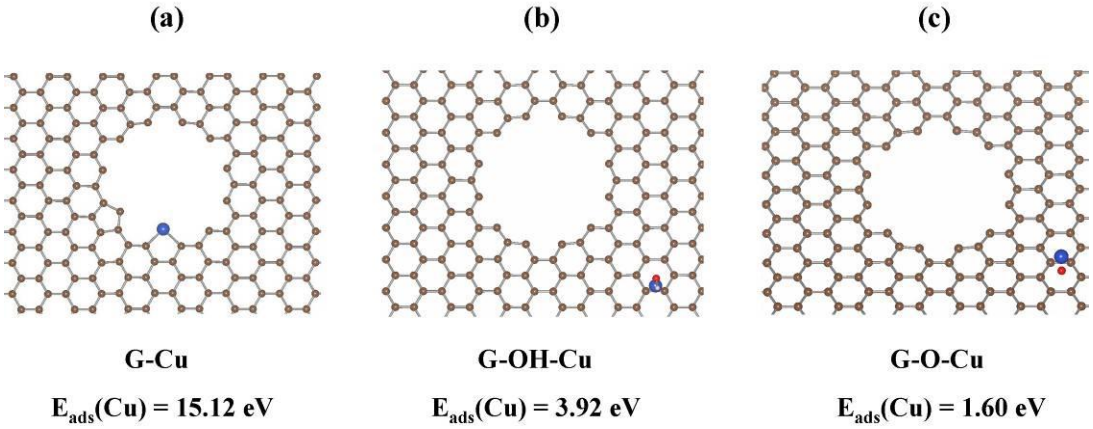

Fig. S4 (a) Cu adsorbed on the defect of GO; (b) Cu adsorbed on the –OH group of the GO surface; (c) Cu adsorbed on the –O– group of the GO surface.

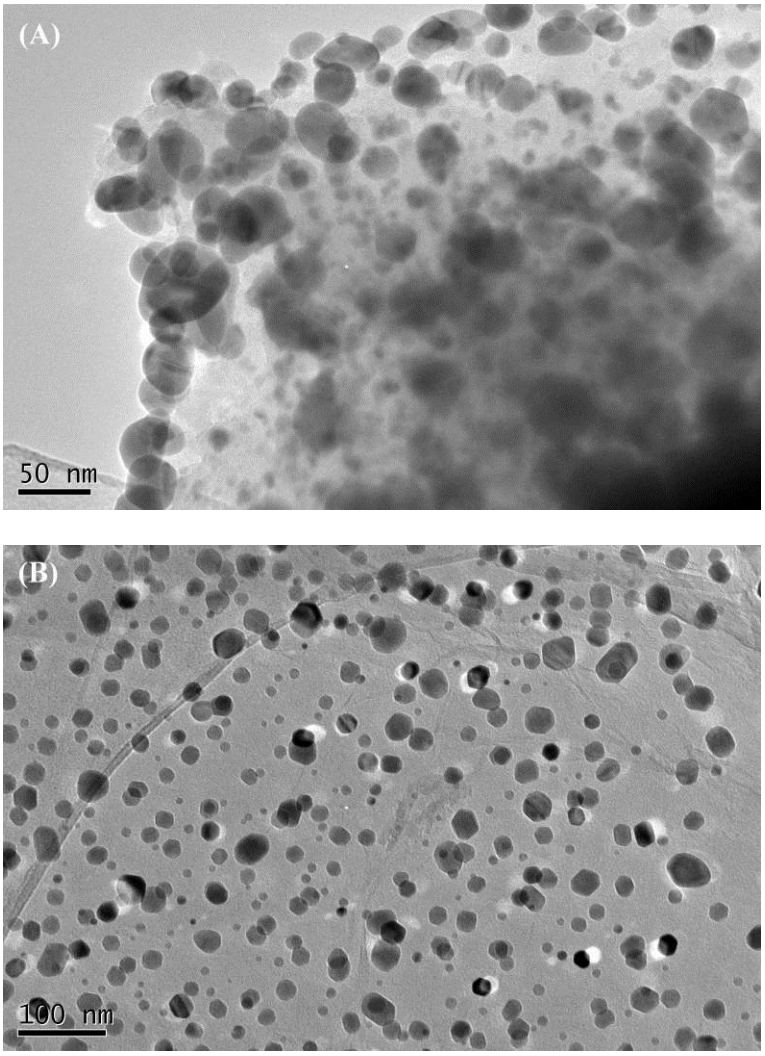

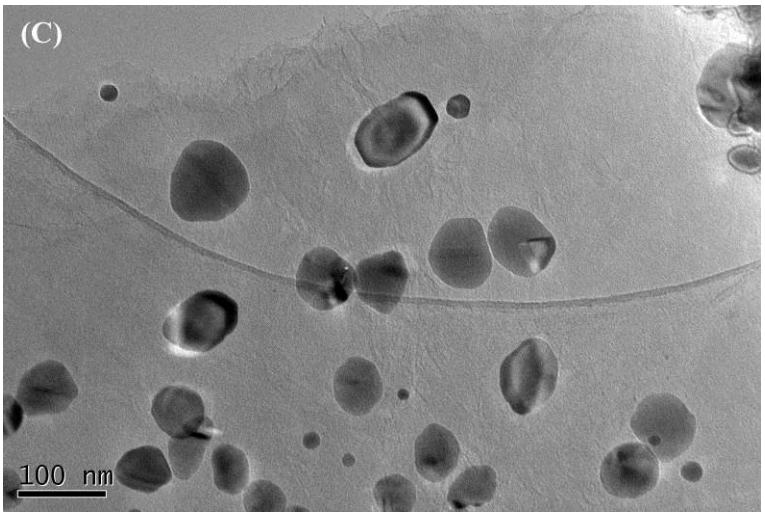

Fig. S5 HRTEM images of (A) CG-3,(B) CG-9 and (C) CG-15.

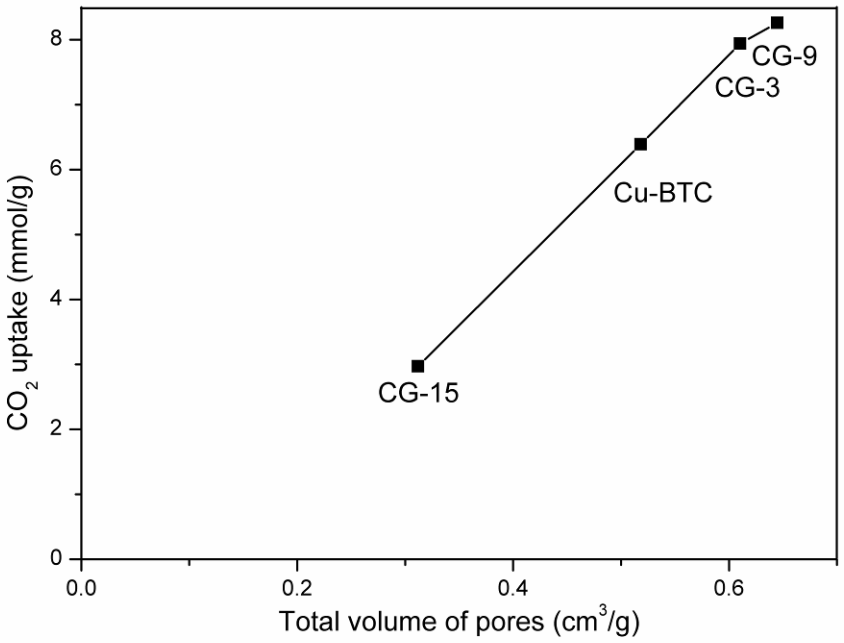

Fig. S6 Carbon dioxide storage plotted against total volume of pores.

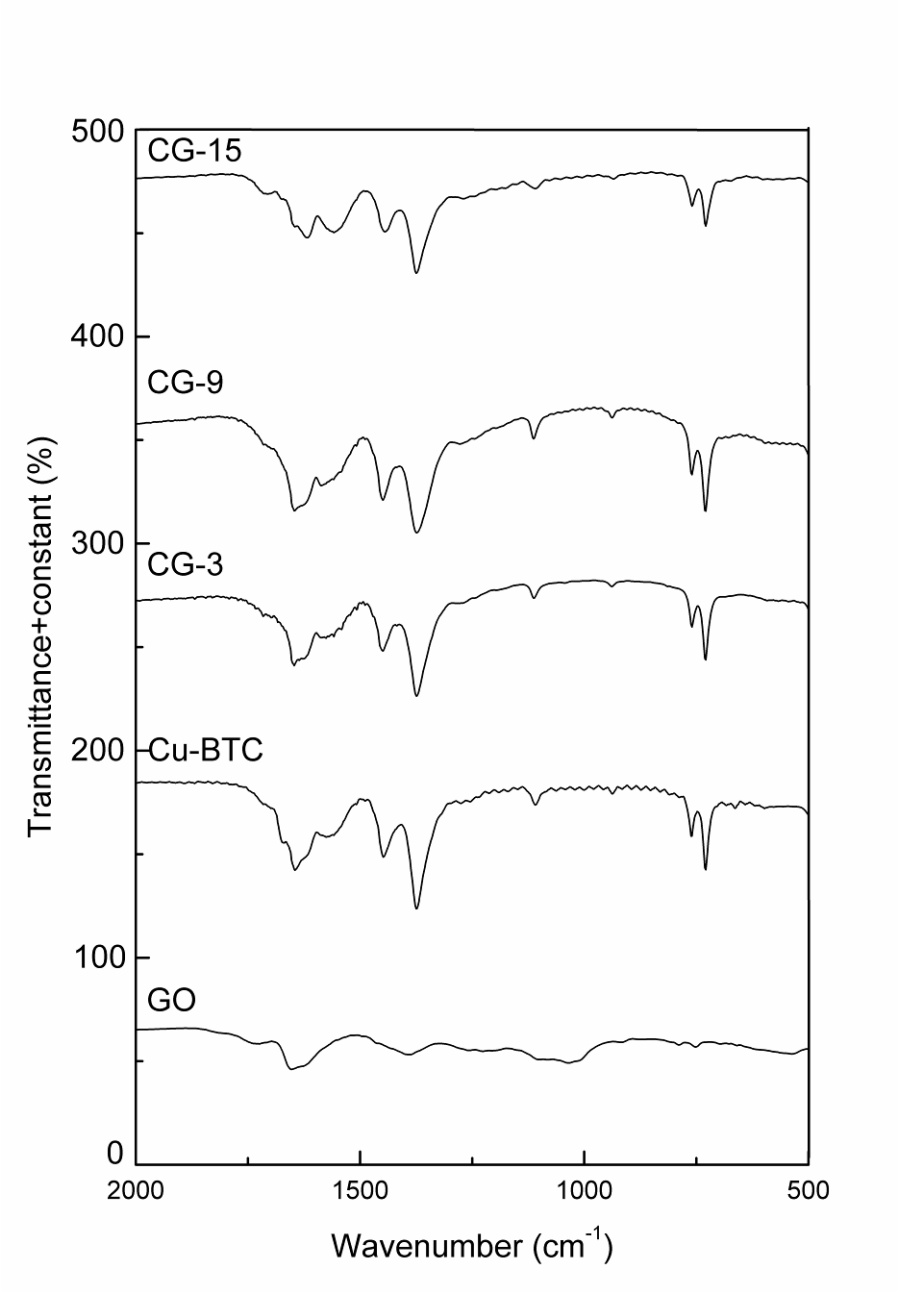

Fig. S7 FT-IR spectra of the parent materials and the composites.

The FT-IR spectra of the materials were recorded. The range above 2000 cm^{-1} does not present features relevant to this analysis, so only the range between 500 and 2000 cm^{-1} is reported. The vibrational peaks of GO are consistent with fingerprint groups such as carboxylic species; hydroxyl species and epoxy species (C=O, 1720-1740 cm^{-1}; OH deformation, ~1390 cm^{-1}; C-O stretching, 1230-1250 cm^{-1}; C-O-C stretching, ~1060 cm^{-1}; C=C from unoxidized sp^2 CC bonds, 1630-1650 cm^{-1}).

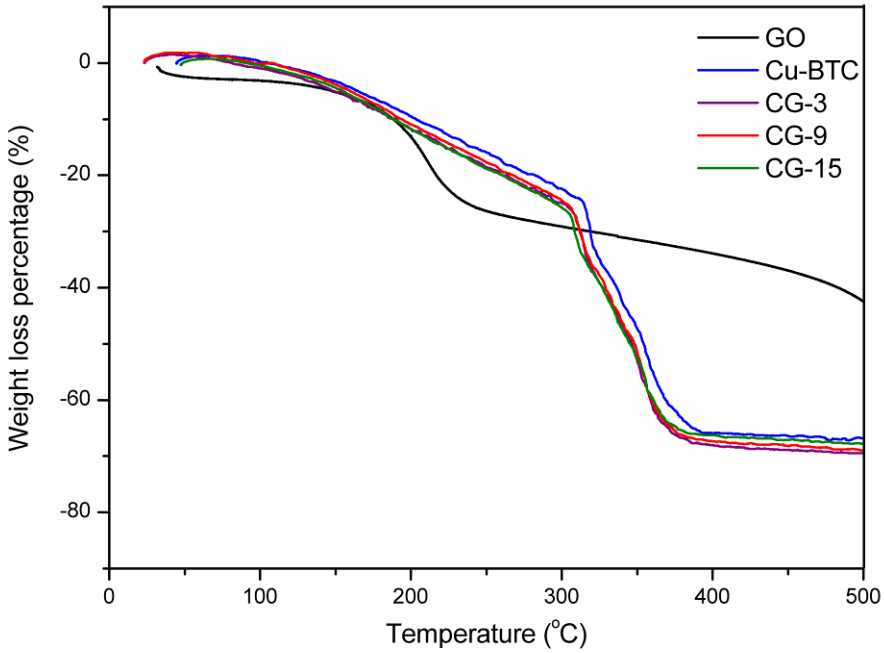

Fig. S8 TGA plots of the parent materials and the composites.

The thermal decomposition of GO can be accompanied by a vigorous release of gas, resulting in a rapid thermal expansion of the material. This is evident by both a large volume expansion and a larger mass loss (from flying GO debris in the TGA instrument) at a rapid heating regime (5 ^{0}C/min). Therefore, we did the TGA experiment of GO at a lower heating regime (1 ^{0}C/min) for precision analysis. The difference of the hypothetical values between weight loss percentage of Cu-BTC and composites can be ignored taking into account the percentage of each component in the composites and the weight loss percentage of GO and Cu-BTC alone. Eq. (1) provides the details of the calculation:

$$X_n = X_{GO} \times wt.\%_{GO} + X_{Cu\text{-}BTC} \times wt.\%_{Cu\text{-}BTC} \quad (1)$$

where "X_n" is the weight loss percentage of composite CG-n to determine, "X_{GO}" and " $X_{Cu\text{-}BTC}$" are the weight loss percentage of GO and Cu-BTC separately, and "$wt.\%_{GO}$" and "$wt.\%_{Cu\text{-}BTC}$" are the weight percentages of GO and Cu-BTC in CG-n.

$X_{Cu\text{-}BTC} - X_{CG\text{-}3}$ =0.73%; $X_{Cu\text{-}BTC} - X_{CG\text{-}9}$ =2.2%; $X_{Cu\text{-}BTC} - X_{CG\text{-}15}$ =3.6%; (X_{GO} = 42.6% and $X_{Cu\text{-}BTC}$ = 66.8% at 500 ^{0}C)

The TGA curves (see below figure) for the composites look rather similar to that of Cu-BTC, but the major weight loss related to the GO in composite is absent. An explanation should be the formation of the composites via interaction between the cupric ions from Cu-BTC and the epoxy groups on the surface of GO, which prevents the decompose of GO at lower temperature.

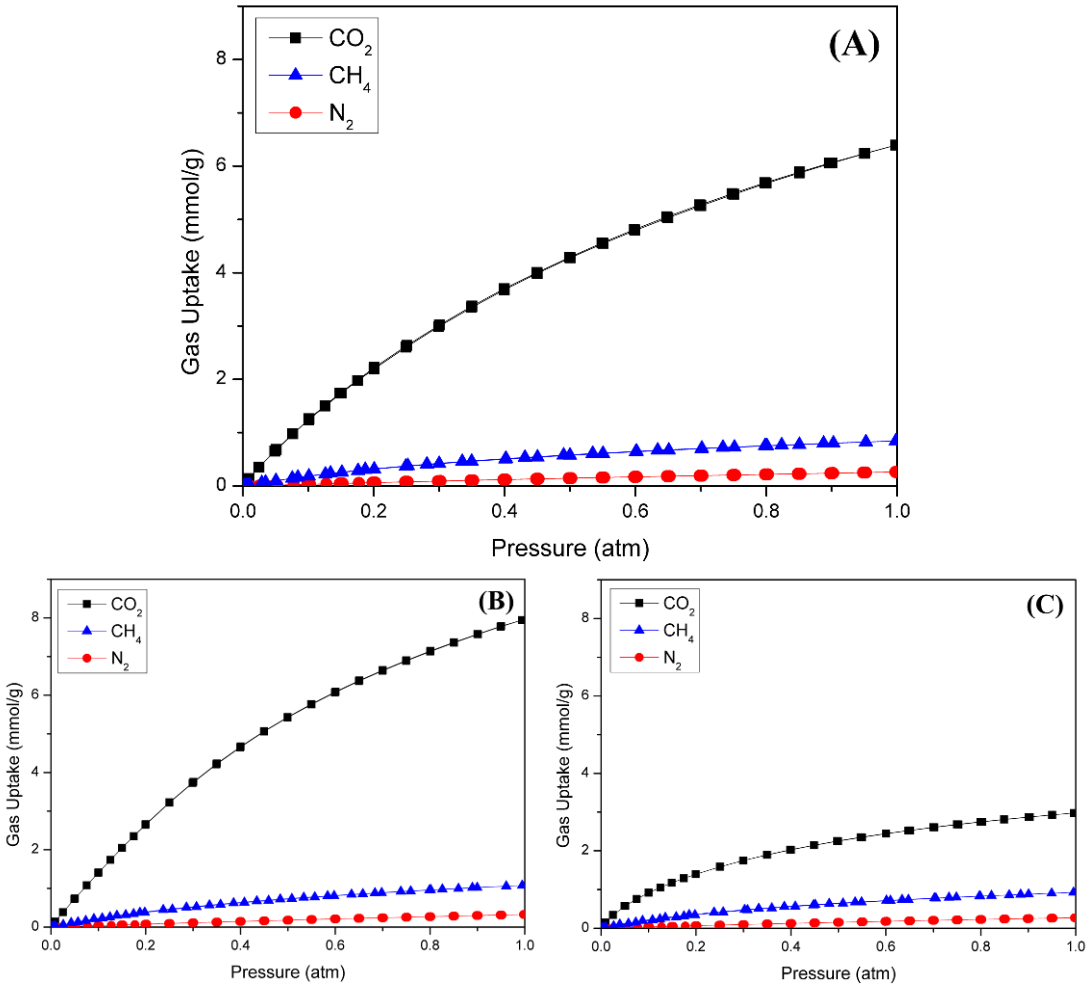

Fig. S9 Adsorption isotherms of Cu-BTC(A), CG-3(B) and CG-15(C) for CO_2, CH_4 and N_2 at 273K.

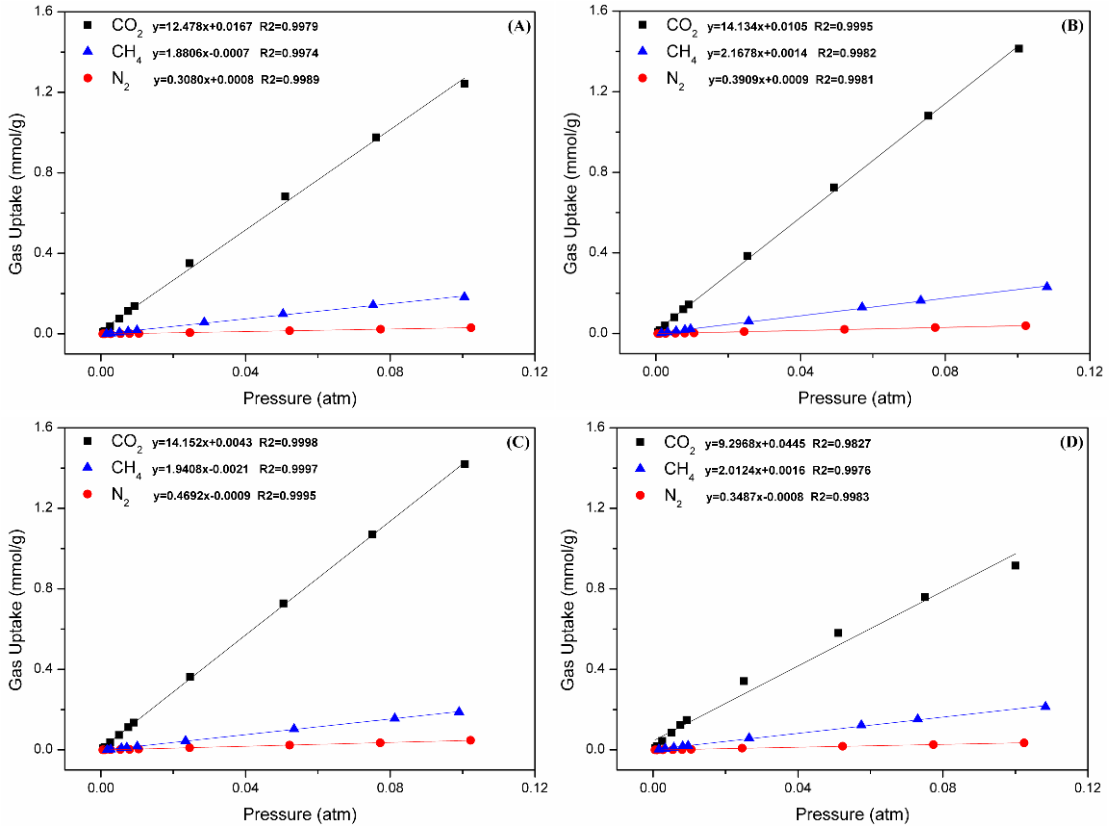

Fig. S10 Initial slope calculation of Cu-BTC (A), CG-3 (B), CG-9 (C) and CG-15 (D) for CO_2, CH_4 and N_2 isotherms collected at 273K.